Near-field scattering of longitudinal fields

Alexandre Bouhelier,[a] Michael R. Beversluis, and Lukas Novotny
The Institute of Optics, University of Rochester, Rochester, New York 14627

(Received 6 March 2003; accepted 5 May 2002)

Longitudinal fields created in strongly focused laser beams are investigated by near-field optical microscopy. Sharp metallic and dielectric tips are raster scanned through the focus of these modes. It is found that regardless of the tip material, the signal scattered by the tip is a measure for the strength of the local longitudinal field. A surprising contrast reversal is observed between the images obtained with a metallic tip and the images obtained with a dielectric tip. The contrast reversal originates from a non-negligible tip–sample interaction. © *2003 American Institute of Physics.* [DOI: 10.1063/1.1586482]

A weakly focused fundamental laser mode is well approximated by a Gaussian beam for which the electric field **E** and the magnetic field **H** are transverse to the axis of propagation. However, for strongly focused laser modes, the paraxial approximation fails and the fields are no longer purely transverse. Near the laser focus, the field vectors can have strong components in the direction of propagation, so-called longitudinal fields. A peculiarity of these fields is that they do not propagate and are confined to the focal region. For some tightly focused higher-order laser modes, the strength of the longitudinal fields can be comparable to or even exceed the strength of transverse fields.[1] Focused higher-order laser modes and the longitudinal fields associated with them have already found applications in various fields. For instance, it was shown that by using the transverse and longitudinal components of the field, the orientation of a single molecular absorption dipole can be determined.[1,2] It was also proposed that the polarization direction of longitudinal fields provides the necessary condition for field enhancement at the apex of a sharp tip used in apertureless scanning near-field optical microscopy.[3] In this letter, we investigate experimentally the spatial distribution of longitudinal fields and demonstrate their role in near-field optical imaging.

For our study we used two well-known field distributions: (i) the focal fields of a fundamental Gaussian beam HG_{00} and (ii) the focal fields of a Hermite–Gaussian HG_{10} laser mode. Far from the focal region, the HG_{10} mode is characterized by two lobes with polarizations pointing from one lobe to the other. The fields in the two lobes are 180° out of phase with respect to each other.

In order to study the field distribution of these two laser modes, sharp metallic and dielectric tips are scanned through the focal regions. The tips act as nanoscopic scatterers for the electric field. By recording the scattering signal as a function of the tip position within the focal region we can map out the spatial variations of the scattering strength as schematically shown in Fig. 1(a).

The metal tips are produced by electrochemically etching a 100-μm-thick gold wire. The wire is dipped in a HCl solution and an alternating current is applied between the gold wire and an immersed platinum electrode. Typical tip diameters are 20 to 30 nm, with a cone angle of 30° as checked by scanning electron microscopy. Alternatively, sharp glass-fiber tips are produced following the technique introduced by Stöckle *et al.*[4] Typical diameters of the glass tips are 30 nm, with a full cone angle of 25°.

The experimental setup is sketched in Fig. 1(b). The excitation source is a cw Ti sapphire laser working at a wavelength of 830 nm. A Gaussian HG_{00} beam was produced by spatially filtering the laser beam with a 25-μm pinhole. Alternatively, a phase plate can be adjusted in the beam path to produce a HG_{10} mode. The phase plate consists of two halves, with one half-overcoated with an SiO_2 layer such that a π phase shift between the two parts of the beam is introduced.[3] The beams are then directed on an unpolarized 50/50 beam splitter and focused on the surface of a cover slip by an oil-immersion objective [numerical aperture (NA):1.4]. In our experiment, a tip is brought in the immediate vicinity of a glass cover slip by means of shear-force regulation,[5] and is scanned laterally through the focal region. The scattered light is collected by the same objective and directed on an avalanche photodiode. An image of the laser

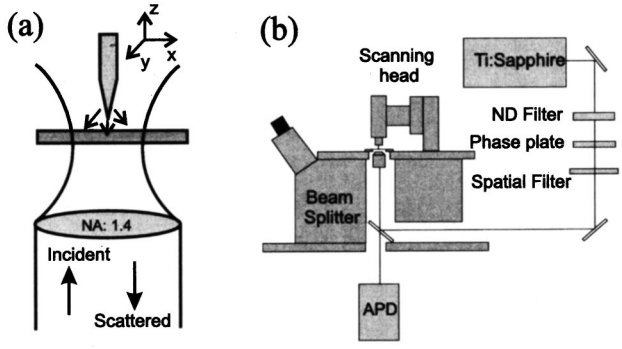

FIG. 1. (a) Principle of the near-field scattering experiments. A tip is scanned through a tightly focused laser beam and the backscattered light is recorded as a function of the tip position (x,y). (b) Schematic of the experimental setup. A phase plate and a spatial filter are used to convert the mode of Ti:sapphire laser to a Gaussian HG_{00} mode or a Hermite–Gaussian HG_{10}. The laser beam is deflected by a 50/50 beam splitter and focused by a 1.4-NA objective on the surface of a glass cover slip. A scanning head, supporting the tips, is placed on the top of our microscope. Backscattering light is collected by the same objective, and sent to an avalanche photodiode.

[a]Electronic mail: bouhelie@optics.rochester.edu

 © 2003 American Institute of Physics
Downloaded 10 Oct 2003 to 128.151.240.170. Redistribution subject to AIP license or copyright, see http://ojps.aip.org/aplo/aplcr.jsp

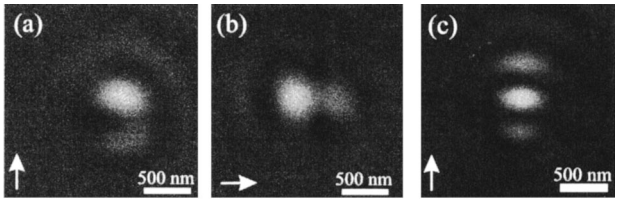

FIG. 2. Scan images recorded with a gold tip. A Gaussian excitation beam is used in (a) and (b), and a Hermite-Gaussian (1,0) beam mode is used in (c). The arrows indicate the direction of the incident polarization. A 90° polarization rotation leads to a rotation of the recorded pattern [(a) and (b)]. Images are 2×2-μm in size.

focus is obtained by correlating the detected scattering signal with the tip position.

Figures 2(a) and 2(b) show the recorded images when a gold tip is scanned through the focal spot of a Gaussian beam. The scan range is 2×2 μm for both images. The pattern in Fig. 2(a) shows two bright lobes oriented vertically in the polarization direction. The lobes are surrounded by a constant background that originates from the back-reflected laser beam. The longitudinal field generates a signal that is a factor of 2 stronger than the background. As shown in Fig. 2(b), a 90° rotation of the polarization direction results in a 90° rotation of the scattering image. The observed asymmetry between the two lobes is independent of the incoming polarization direction, indicating that its origin is associated with the quality of the Gaussian beam and/or the quality of the focus rather than by the shape of the tip. We also find that the recorded patterns depend sensitively on the relative position of the focus to the interface.[6]

Using the same gold tip, we recorded the scattered signal when a Hermite–Gaussian HG_{10} beam was focused as shown in Fig. 2(c). A central bright region surrounded by two less intense spots oriented along the polarization direction can be recognized. A second set of lobes is barely visible in the image. The count rate at the central lobe location is increased by a factor of 2.3 as compared to the back-reflected signal.

To understand the recorded patterns, we performed an angular spectrum analysis of the focal fields taking into account the reflection and transmission coefficients at the air/glass interface.[1,6,7] The calculated intensity of the longitudinal field $|\mathbf{E}_z|^2$ is shown in Figs. 3(a) and 3(b) for a focused HG_{00} and HG_{10}, respectively. Figure 3(a) displays two bright lobes of equal intensity and oriented along the polarization direction that are very similar to our experimental finding of Fig. 2(a). The theoretical and experimental images for the HG_{10} mode show also good agreement [cf., Figs. 2(c) and 3(b)]. We therefore conclude that the contrast in the scattered images is due to scattering of longitudinal fields and that the gold tip is sensitive to the longitudinal component of the focal field.

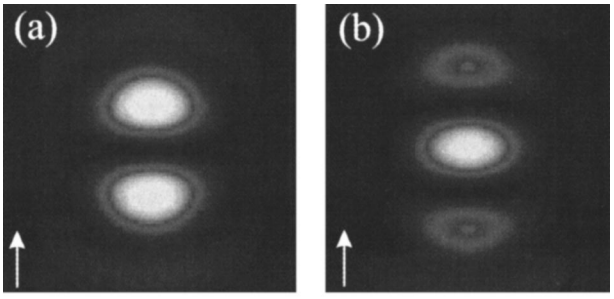

FIG. 3. Calculated spatial distribution of the longitudinal field $|\mathbf{E}_z|^2$ in the focal plane of a Gaussian beam (a) and of a Hermite–Gaussian (1,0) beam (b). Image size is 1.5×1.5 μm. A scaling factor ($3\times$) was introduced in (a) to match the intensity level of (b).

To understand the interaction between tip and field, we model the tip's response by an effective dipole $\mathbf{p}(\omega)$ located at the center of the tip apex. The dipole is induced by the exciting field $\mathbf{E}_o$ in absence of the tip, and can be written as

$$\mathbf{p}(\omega)=\begin{bmatrix}\alpha_\perp & 0 & 0\\ 0 & \alpha_\perp & 0\\ 0 & 0 & \alpha_\parallel\end{bmatrix}\mathbf{E}_o(\omega), \tag{1}$$

where we chose the z-axis to coincide with the tip axis. $\alpha_\perp$ and $\alpha_\parallel$ denote the transverse and longitudinal polarizabilities, respectively, defined by

$$\alpha_\perp(\omega)=4\pi\varepsilon_o r_o^3\frac{\varepsilon(\omega)-1}{\varepsilon(\omega)+2},\ \text{and}$$

$$\alpha_\parallel(\omega)=8\pi\varepsilon_o r_o^3 f_e(\omega). \tag{2}$$

$\alpha_\perp$ is the well-known quasistatic polarizability of a small sphere, ε denotes the bulk dielectric constant of the tip, and r_o is the tip radius. The longitudinal polarizability $\alpha_\parallel$ follows from the requirement that the field at the end of the tip is identical to the computationally determined value of the field $[\mathbf{E}(0,0,r_o)=f_e\mathbf{E}_o]$. Here, f_e is the numerically determined complex field-enhancement factor. Using the multiple-multipole program to solve for the electromagnetic fields for the three-dimensional tip geometry,[3] we find a value $f_e=-2.9+11.8i$, assuming $\lambda=830$ nm. Once the tip dipole is determined, the electric field $\mathbf{E}$ in the vicinity of the tip is calculated as

$$\mathbf{E}(\mathbf{r},\omega)=\mathbf{E}_o(\mathbf{r},\omega)+\frac{1}{\varepsilon_o}\frac{\omega^2}{c^2}\mathcal{G}(\mathbf{r},\mathbf{r}_o,\omega)\mathbf{p}(\omega), \tag{3}$$

where $\mathbf{r}_o$ specifies the origin of $\mathbf{p}$ and $\mathcal{G}$ is the dyadic Green's function. The detected scattered power is proportional to the square of the field $\mathbf{E}$ evaluated in the far-field. We note that if the field-enhancement factor f_e is larger than the fractional term in the expression of $\alpha_\perp$, the main contributing term to the scattered power is given by a dipole oriented along the tip axis. In this case, the strength of the scattered longitudinal field exceeds the strength of the transverse field, which is exactly the situation encountered in our experiments using a gold tip. Thus, the outlined theory explains the good agreement between the recorded images and the calculated maps of $|\mathbf{E}_z|^2$.

In a next step, we performed the same experiments using a glass tip. Figures 4(a) and 4(b) show the recorded scattered signal when the dielectric tip is scanned through the focal region of the HG_{00} beam. The polarization direction is along the direction of the two lobes. The shape of the patterns is similar to the calculated ones in Fig. 3 and to those measured using a gold tip. However, an unexpected contrast reversal is observed between the images recorded with the glass tip and the images recorded with a gold tip. We observed a depletion of ~15% of the scattering signal whenever the tip is aligned with the longitudinal field.

Downloaded 10 Oct 2003 to 128.151.240.170. Redistribution subject to AIP license or copyright, see http://ojps.aip.org/aplo/aplcr.jsp

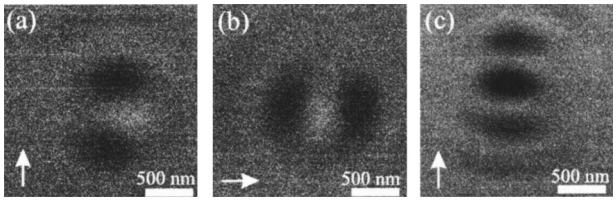

FIG. 4. Scan images recorded with a glass tip. A Gaussian excitation beam is used in (a) and (b), and a Hermite-Gaussian (1,0) beam mode is used in (c). The arrows indicate the direction of the incident polarization. A 90° polarization rotation leads to a rotation of the recorded pattern [(a) and (b)]. A contrast reversal is observed compared with Fig. 2. Images are 2 $\times 2$-μm in size.

As shown in Fig. 4(c), the same phenomenon is observed for the HG_{10} mode. We can even recognize in Fig. 4(c) a second set of outer lobes that are barely visible in the images acquired with a gold tip. Here, a signal reduction of 30% is measured on top of the central lobe. We investigated several possibilities to explain the contrast reversal. On one hand, the backscattered light can be reduced by coupling to a waveguide mode of the fiber tip. In this case, the coupling should be strongest when the tip is excited by the transverse field, which possesses the same angular symmetry as the propagating fiber mode. However, Figs. 4(a)–4(c) show that the backscattered signal is weakest when the tip is facing the longitudinal field, ruling out the fiber coupling mechanism. We also checked the angular dependence of the backscattered light to ensure that light within the critical angle (allowed light) exhibits the same effect as light emitted beyond the critical angle (forbidden light).[8] The most plausible explanation is that the dielectric tip acts as a local index-matched medium, that is, it attracts the fields depending on the polarizability of the tip. This effect has already been observed in early simulations of near-field optical microscopy.[9] Since for a dielectric tip, $\alpha_{\parallel}$ is slightly larger than $\alpha_{\perp}$, the tip will favorably attract longitudinal fields and deplete the backscattered radiation whenever the tip is faced by a local longitudinal field.

To support our observations, we repeated the experiments by replacing the tips by small spherical particles for which $\alpha_{\parallel}=\alpha_{\perp}$. For a glass particle we find a negative contrast in the scattered images with a pattern that resembles the total field $|\mathbf{E}_o|^2$ rather than the longitudinal field $|\mathbf{E}_z|^2$. Similarly, a gold particle renders the same pattern, but with a positive contrast.

Our observations have important consequences for near-field optical microscopy. First, we clearly demonstrated that the recorded images do not coincide with the total field distribution $|\mathbf{E}_o|^2$ in absence of the tip. Instead, the measured contrast is generated by the tip–field interaction driven by the longitudinal field $\mathbf{E}_z$, whether the tip is dielectric or metallic. In the case of a gold tip, the optical response can be accurately modeled by a dipole oriented along the main tip axis. The strength of the dipole, that is, the strength of the scattered signal, is an indirect measure of the field enhancement produced at the end of the tip. Second, we showed that the field-enhancement factor can be optimized by using laser modes with strong longitudinal fields as excitation sources. Third, since the transmission of the laser beam through the interface can be influenced by a sharp tip, we found that the tip cannot be approximated by a purely passive probe, as is commonly assumed in theoretical investigations. Finally, we found that different information about a near-field distribution can be retrieved by scanning tips and particles. While a tip renders information about the longitudinal field distribution, a particle is predominantly sensitive to the total field strength. Subsequent imaging with a tip and a particle brings new opportunities for characterizing field distributions near nanoscale structures.

This research was funded partially by a fellowship from the Swiss National Science Foundation (A.B.) and by NSF grant No. DMR-0078939.

[1] L. Novotny, M. R. Beversluis, K. S. Youngworth, and T. G. Brown, Phys. Rev. Lett. **86**, 5251 (2001).
[2] B. Hecht, B. Sick, and L. Novotny, Phys. Rev. Lett. **85**, 54482 (2000).
[3] L. Novotny, E. J. Sànchez, and X. Sunney Xie, Ultramicroscopy **71**, 21 (1998).
[4] R. Stöckle, Ch. Fokas, V. Deckert, R. Zenobi, B. Sick, B. Hecht, and U. P. Wild, Appl. Phys. Lett. **75**, 160 (1999).
[5] K. Karrai and D. R. Grober, Appl. Phys. Lett. **66**, 1842 (1995).
[6] L. Novotny, D. R. Grober, and K. Karrai, Opt. Lett. **26**, 789 (2001).
[7] D. P. Biss, and Th. G. Brown, Opt. Express **9**, 490 (2001).
[8] B. Hecht, H. Bielefelt, D. W. Pohl, L. Novotny, and H. Heinzelmann, J. Appl. Phys. **84**, 5873 (1998).
[9] L. Novotny, D. W. Pohl, and P. Regli, J. Opt. Soc. Am. A **11**, 1768 (1994).

Downloaded 10 Oct 2003 to 128.151.240.170. Redistribution subject to AIP license or copyright, see http://ojps.aip.org/aplo/aplcr.jsp